Numerical modelling of swelling and shrinking soils around slabs-on-ground

Delwyn G. Fredlund and Hung Q. Vu
Department of Civil and Geological Engineering, University of Saskatchewan, Saskatoon, SK, Canada

Abstract: This paper presents a technique to analyze the problems associated with swelling and shrinking soils around slabs-on-ground constructed on expansive soils. The technique makes use of two numerical models (i.e., saturated/unsaturated seepage model and stress/deformation model). The saturated/unsaturated seepage model is used to predict matric suction conditions in the soil with respect to time under specified flux boundary conditions. The stress/deformation model is then used to predict the displacements and resulting stresses from changes in applied load and matric suction. The analysis also provides the bending stresses and moments along the slab.

INTRODUCTION

Residential foundations such as slabs-on-ground are often constructed on unsaturated, expansive soils and have to resist deformation associated with external loads and changes in matric suction in the soil. Residential foundations are lightly loaded, and therefore the displacements are mostly due to changes in matric suction. Changes in matric suction can occur as a result of variation in climatic conditions, change in depth of water table, water uptake by vegetation, removal of vegetation or the excessive watering of a lawn.

The soil beneath an impervious cover can deform into either an edge drop mode or an edge lift mode (Fig. 1). Edge drop occurs when the matric suction in the soil surrounding the slab gradually increases due to evaporation and/or transpiration. Soil volume decreases more around the perimeter of the slab than under the interior of the slab, because the soil around the slab becomes dryer than the soil beneath the cover. In reverse, edge lift occurs when the matric suction in the soil decreases due to the infiltration of water in to the soil mass around the slab.

This paper presents a methodology to simulate the edge lift (i.e., swelling) and edge drop (i.e., shrinkage) problems around a somewhat flexible impervious cover (or a uniform thickness slab) placed on an unsaturated, expansive soil. A two-dimensional example problem involving a flexible impervious cover (or a slab-on-ground) is used to illustrate the suggested methodology for predicting swelling and shrinking behavior. Three scenarios are analyzed. The first scenario presents an analysis associated with the edge drop mode around a flexible cover due to evaporation at the uncovered ground surface. The second scenario presents an analysis associated with the edge lift mode around a flexible cover. The edge lift mode is simulated by allowing water to infiltrate into soil mass from the uncovered ground surface. The third scenario presents an analysis of edge lift of a constant thickness concrete slab.

THEORY

Two variables are required to describe the stress state of an unsaturated soil; namely, net normal stress, $(\sigma - u_a)$ and matric suction, $(u_a - u_w)$, where σ is net total stress, u_a is pore-air pressure, and u_w is pore-water pressure (Fredlund and Morgenstern, 1977). For typical engineering problems, pore-air pressure is generally constant and equal to atmospheric pressure, while pore-water pressure is negative relative to pore-air pressure. Volume change in an unsaturated soil can occur as a result of changes in each or both of these stress state variables.

The solution of a swelling or shrinking soil problem associated with unsaturated, expansive soil involves the solution of a saturated/unsaturated seepage model and a stress/deformation model. The models can be formulated based on the general theory of unsaturated soil behaviour. A two-dimensional problem will be used for illustration purposes in this paper, but the model can readily be extended to three-dimensions.

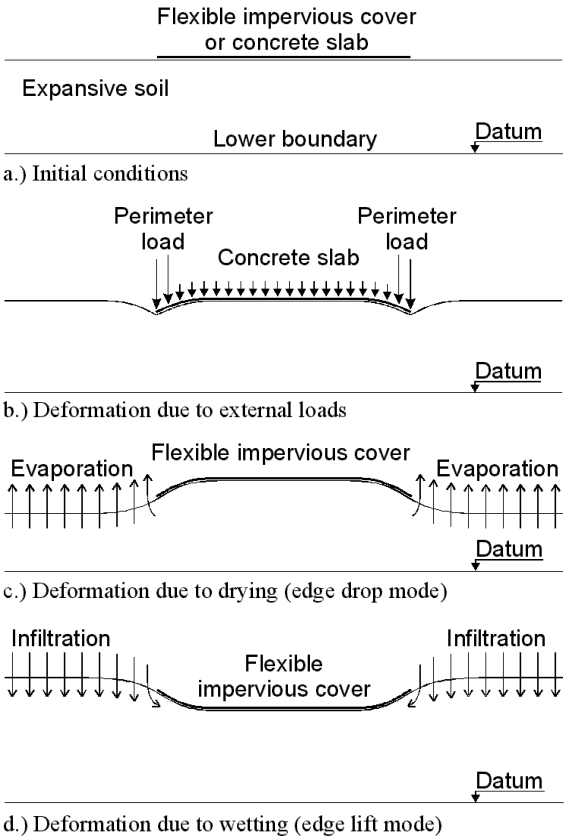

Figure 1. Illustration of the soil response to external loads and changes in matric suctions (after Post-tensioning Institute, 1996)

Saturated/unsaturated seepage model

The governing partial differential equation for water flow through a heterogeneous, anisotropic, saturated/unsaturated soil can be derived by satisfying conservation of mass for a representative elemental volume. It is assumed that flow follows Darcy's law with a non-linear coefficient of permeability function. If it is assumed that the total stress remains constant during a transient process and that pore-air pressure is atmospheric, the differential equation can be written as follows for two-dimensional, transient, saturated-unsaturated seepage (Fredlund and Rahardjo, 1993):

$$\frac{\partial}{\partial x}\left(k_x \frac{\partial h}{\partial x}\right)+\frac{\partial}{\partial y}\left(k_y \frac{\partial h}{\partial y}\right)=m_2^w \gamma_w \frac{\partial h}{\partial t} \tag{1}$$

where: h = total head (i.e., pore-water pressure head plus elevation head); k_x and k_y = coefficient of permeability of the soil in the x- and y-direction, respectively; γ_w = the unit weight of water (i.e., 9.81 kN/m^3), m_2^w = the slope of the soil-water characteristic curve.

Both the coefficient of permeability and coefficient of water storage are dependent on stress states in soils (i.e., net normal stress and matric suction). However, both coefficients for an unsaturated soil are predominantly a function of the matric suction.

The water storage coefficient indicates the amount of water taken on or released by the soil because of a change in the pore-water pressure and can be represented by the slope of the soil-water characteristic curve. Therefore, the water storage function is obtained by differentiating the soil-water characteristic curve with respect to matric suction (Fredlund and Xing, 1994). Numerous equations have been proposed to simulate the soil-water characteristic curve (Gardner, 1958; van Genuchten, 1980; Fredlund and Xing, 1994). The soil-water characteristic curve described in the present study is limited to the Fredlund and Xing (1994) equation. The Fredlund and Xing (1994) equation is shown below:

$$\theta = \theta_s \left[\frac{1}{\ln\left(e+(\psi/a)^n\right)}\right]^m \tag{2}$$

where: ψ = soil suction (kPa), e = natural log base, 2.71828..., θ_s = volumetric water content at saturation, a = a soil parameter which is related to the air entry value of the soil (kPa), n = a soil parameter which controls the slope at the inflection point in the soil-water characteristic curve, and m = a soil parameter which is related to the residual water content of the soil.

There are several coefficient of permeability equations that have been proposed to represent the permeability function of an unsaturated soil (e.g., Gardner, 1958; Fredlund et al., 1994; Leong and Rahardjo, 1997). These equations involve finding best-fit parameters, which produces a curve that fits the measured data. The equation proposed by Leong and Rahardjo (1997) is used to describe the permeability function for transient water flow analysis in this paper. Leong and Rahardjo (1997) illustrated that the coefficient of permeability is a power function of volumetric water content. Using the Fredlund and Xing (1994) equation, the permeability function was shown to take the following form:

$$k = k_s \left[\frac{1}{\ln\left(e+(\psi/a)^n\right)}\right]^{mp} \tag{3}$$

The parameter p can be determined by using a curve fitting of the coefficient of permeability data.

The transient water flow equation (Eq. 1) along with the equation of a soil-water characteristic curve (Eq. 2) and a permeability function (Eq. 3), can be used to predict pore-water pressure profiles (i.e., suction profiles) at different times during a seepage process. The suction profiles can then be used to compute the suction change for the stress/deformation analysis. The deformations due to changes in suction during any time period can then be predicted by specifying the initial and final soil suction profile.

The solution for transient saturated-unsaturated seepage requires the definition of initial soil suction conditions, the saturated-unsaturated soil properties in terms of a permeability function and a water storage function, as well as the moisture flux boundary conditions. The results of the seepage analysis provide the distributions of soil suction in the soil profile with respect to time for the specified boundary conditions.

Stress/deformation model

The governing partial differential equations in term of displacements in the x- and y-direction (i.e., u and v) for plane strain loading ($d\varepsilon_z = 0$) of an isotropic, non-linear elastic soil can be written as follows (Hung and Fredlund, 2000):

$$\frac{\partial}{\partial x}\left\{c\left[(1-\mu)\frac{\partial u}{\partial x}+\mu\frac{\partial v}{\partial y}-\frac{(1+\mu)}{H}(u_a-u_w)\right]\right\} + \frac{\partial}{\partial y}\left\{G\left(\frac{\partial v}{\partial x}+\frac{\partial u}{\partial y}\right)\right\}=0 \tag{4}$$

$$\frac{\partial}{\partial x}\left\{G\left(\frac{\partial v}{\partial x}+\frac{\partial u}{\partial y}\right)\right\}+ \frac{\partial}{\partial y}\left\{c\left[\mu\frac{\partial u}{\partial x}+(1-\mu)\frac{\partial v}{\partial y}-\frac{(1+\mu)}{H}(u_a-u_w)\right]\right\}+\rho g=0 \tag{5}$$

where: E = elasticity parameter for the soil structure with respect to net normal stress; H = elasticity parameter for the soil structure with respect to matric suction; μ = Poisson's ratio for the soil structure; ρ = density of the soil; g = acceleration due to gravity; $c=\frac{E}{(1-2\mu)(1+\mu)}$; and $G=\frac{E}{2(1+\mu)}$

Equations (4) and (5) can be used to compute the displacements in horizontal and vertical directions under an applied load and/or due to changes in matric suction.

The solution of the stress/deformation model under specified boundary conditions requires the definition of the initial matric suction, initial stress conditions, the elasticity parameter functions associated with the volume change of the soil, and the results from a seepage analysis (i.e., for changes in soil suction).

Initial matric suction can be measured using field methods, laboratory methods (Fredlund and Rahardjo, 1993) or estimated from theoretical considerations of unsaturated soil conditions.

Vertical net normal stresses can be estimated from total unit weight of the soil by total stress theory. Horizontal net normal stress can be estimated from the vertical stresses and the coefficient of earth pressure at-rest, K_0. The estimation of the coefficient of earth pressure at-rest has been presented in Fredlund and Rahardjo (1993), Lytton (1995) and Lytton (1997). Lytton (1997) suggested that the coefficient of lateral earth pressure at-rest, K_0, equal to 0.67 can be used for wetting path; and K_0 equal to 0.33 can be used for drying path.

The elasticity parameters are functions of the stress state of the soil (i.e., net normal stress and/or matric suction). These elasticity parameter functions can be calculated from the void ratio constitutive surface with an assumed value of Poisson's ratio. An entire void ratio constitutive surface can be measured or estimated from the swelling indices, C_s, subject to changes in net normal stress, and C_m, subject to changes in matric suction (Hung, 2003). A typical semi-logarithmic plot of a void ratio constitutive surface for an unsaturated, expansive soil is presented in Fig. 2.

The results of the stress/deformation analysis include the distribution of horizontal and vertical displacements and resulting stresses that occur due to changes in applied load and matric suction.

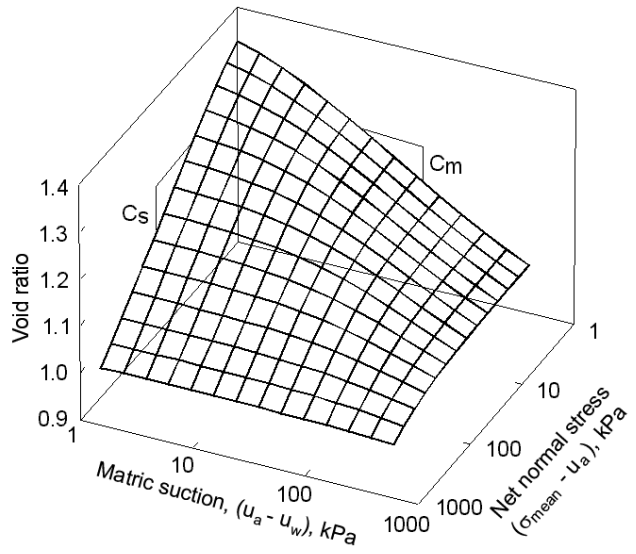

Figure 2. A typical void ratio constitutive surface

Calculation of moments and shear forces in the slab

Assuming that displacements at the edge of the slab are small in comparison to its thickness, the loads applied on the slab can be assumed to be normal to the slab surface. The bending moments can be calculated from the displacements or bending stresses, and the shear force can be calculated from the moments. Timoshenko and Woinowsky-Krieger (1959) presented the following equations for computing bending moments and shear.

$$M = -\frac{E_c h_s^3}{12(1-\mu_c^2)}\frac{\partial^2 v}{\partial x^2} \tag{6}$$

or

$$M = \frac{\sigma_{\max} h_s^2}{6} \tag{7}$$

$$Q = \frac{\partial M}{dx} \tag{8}$$

where: v = vertical displacement of the slab; M = bending moment per unit length; Q = shear force per unit length; h_s = thickness of the slab; σ_{max} = maximum bending stress; E_c = elastic modulus of concrete; and μ_c = Poisson's ratio of concrete.

EXAMPLE PROBLEM AND ANALYSIS RESULTS

The example problem considers the hypothetical case of a 3-meter layer of expansive soil below a 12-meter wide flexible, impervious cover or a concrete slab. It is assumed that a constant matric suction of 400 kPa exists at the 3-meter depth, and there is no change in matric suction below this depth. Because of geometrical symmetry, only half of the geometry is considered for analysis (Fig. 3).

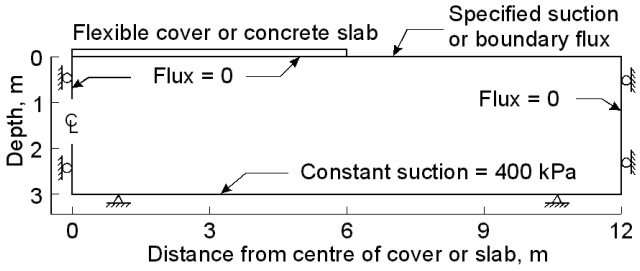

Figure 3. Illustration of the example problem, boundary conditions for seepage and stress-deformation analysis

Three scenarios are analyzed. The first scenario presents the analysis of the edge drop mode associated with a flexible cover due to evaporation at the ground surface outside the cover. The second scenario presents the analysis of the edge lift mode associated with a flexible cover. The edge lift is simulated by allowing water to infiltrate into soil mass from ground surface. The third scenario presents the analysis of edge lift of a constant thickness concrete slab.

Figure 3 shows boundary conditions for the seepage analysis. A matric suction of 400 kPa is specified at the lower boundary. The transient wetting or drying process is induced by specifying a boundary flux (i.e., rate of infiltration or evaporation) or a matric suction at ground surface outside of the cover. A moisture flux equal to zero is specified elsewhere along the boundaries.

Boundary conditions for the stress-deformation analysis are also presented in Fig. 3. The soil is free to move in the vertical direction and fixed in horizontal direction at the left and right sides of the domain. The lower boundary is fixed in both directions.

Details concerning the initial stress and matric suction conditions are presented in the following sections for each of the scenarios.

Soil properties for the seepage analysis are presented in Table 1. The soil-water characteristic curve is described using the Fredlund and Xing (1994) equation, with the parameters a equal to 300 kPa, n equals 1.5 and m equals 1. The permeability func-

tion is described using the equation proposed by Leong and Rahardjo (1997) based on the Fredlund and Xing (1994) equation for the soil-water characteristic curve with p equal to 1. The soil-water characteristic curve and the permeability function are presented graphically in Fig. 4.

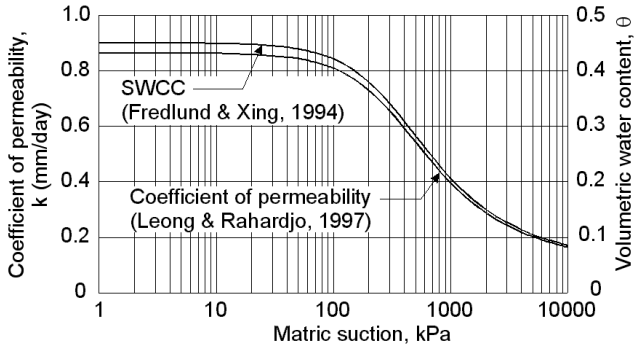

Figure 4. Coefficient of permeability function and soil-water characteristic curve

Table 1. Assumed soil properties for seepage analysis

Soil properties	Values
Coefficient of permeability at saturation, k_s	$1x10^{-8}$ m/day
Volumetric water content at saturation, θ_s	0.45
Parameters for SWCC [Fredlund and Xing (1994)] and permeability function [Leong and Rahardjo (1997)]	a = 300 kPa n = 1.5 m = 1 p = 1

Soil properties for the stress/deformation analysis are presented in Table 2. The void ratio constitutive surface is estimated from the swelling indices, C_s and C_m, and initial void ratio, e_0. A semi-logarithmic plot of the estimated void ratio surface was presented in Fig. 2. The elasticity parameter functions for the soil structure are calculated from the void ratio constitutive surface using an assumed Poisson's ratio (Hung, 2003). The coefficient of earth pressure at-rest equal to 0.33 and 0.67 are used to determine the initial stress state conditions for the edge drop mode and edge lift mode, respectively.

Table 2. Assumed soil properties for stress analysis

Soil properties	Values
Total unit weight, γ_t	17.2 kN/m^3
Specific gravity, G_s	2.80
Initial void ratio, e_0	1.00
Swelling index, C_s	0.15
Swelling index, C_m	0.13
Swelling pressure, P_s	200 kPa
Poisson's ratio for the soil, μ_s	0.4
Elastic modulus for concrete, E_c	10 MPa
Poisson's ratio for concrete, μ_c	0.15

Edge drop for a flexible impervious cover

The initial suction condition is assumed to be a steady state condition where a suction of 20 kPa is specified at upper boundary and a suction of 400 kPa is specified at lower boundary. The drying process is simulated by applying an upward moisture boundary flux (i.e., the evaporation of 10 mm/day at the uncovered ground surface).

Matric suction conditions at ground surface are presented in Fig. 5 for various times after the evaporation commences. It can be seen that a high suction gradient occurred only about one meter outside the edge of the cover and suction change uniformly elsewhere. Figure 6 presents the matric suction profiles at the edge of the cover for various times. Most of suction change took place near ground surface, and advanced deeper with time. Figure 7 presents the distribution of matric suction in the soil profile after three days of evaporation.

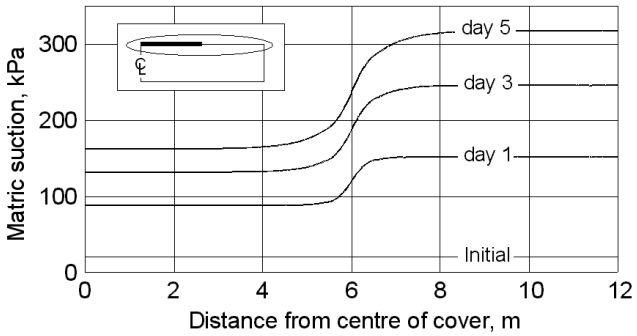

Figure 5. Matric suction at ground surface for various elapsed times of evaporation

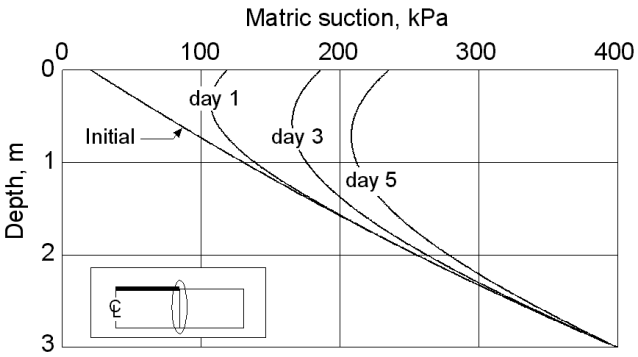

Figure 6. Matric suction profile at the edge of the cover for various elapsed times of evaporation

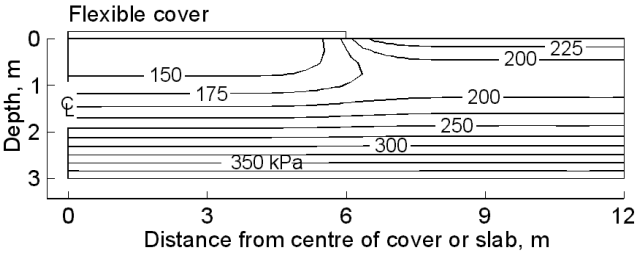

Figure 7. Contours of matric suction after three days of evaporation

Vertical displacements at ground surface are presented in Fig. 8 for various times after the evaporation commences. Differential settlements took place near the edge of the cover. At day 5 about 10 mm of differential settlements was calculated. Figure 9 presents the vertical displacement profiles at the edge of the cover for various times. Figure 10 presents the distribution of vertical dis-

placements in the soil mass after three days of evaporation. Most of the settlements took place near ground surface where the change in matric suction is large and soil has low elastic modulus.

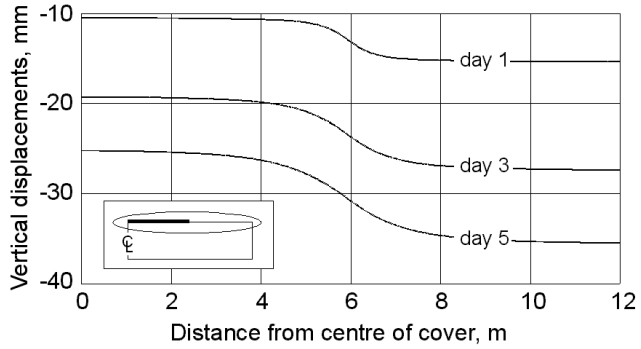

Figure 8. Vertical displacements at ground surface for various elapsed times of evaporation

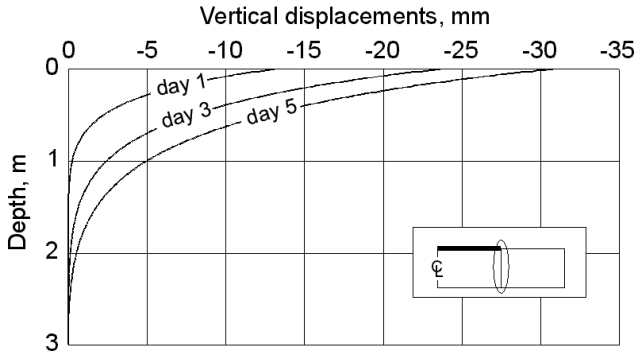

Figure 9. Vertical displacements (i.e., settlements) versus depth at the edge of the cover for various elapsed times of evaporation

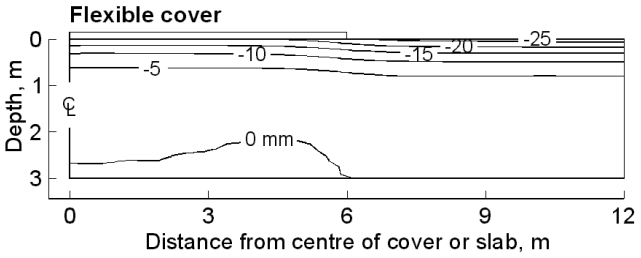

Figure 10. Contours of vertical displacement (i.e., settlements) after three days of evaporation

Edge lift for a flexible impervious cover

The initial suction condition is assumed to be a steady state condition where a zero boundary flux is specified at upper boundary and a suction of 400 kPa is specified at lower boundary. The distribution of initial matric suction is showed in Fig. 11. The wetting process is simulated by allowing water to infiltrate to the soil mass at the uncovered ground surface. Matric suction conditions in the soil mass are analyzed for various infiltration rates (i.e., from 10 mm/day to 60 mm/day), and for the case where zero suction is specified at the uncovered boundary.

Figures 12 and 13 present the matric suction conditions at ground surface and below the edge of the cover, respectively, after one day of infiltration for various infiltration rates. Most of the suction change took place in the uncovered part of the soil profile to a depth of about 1.5 meter and the magnitude of suction change increases as the rate of infiltration increases. After one day of infiltration, the wetting front advanced to a distance of about one-meter from the edge of the slab. No suction change was predicted in soil below the 1.5-meter depth. The maximum change in matric suction was predicted for the case when zero suction was specified at the uncovered part of the boundary.

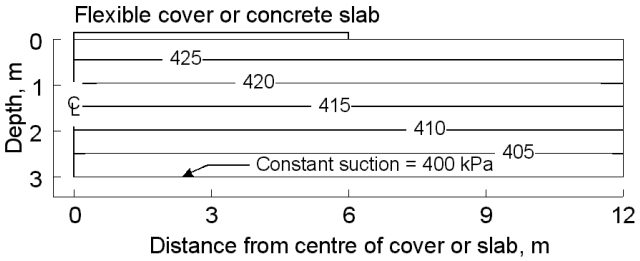

Figure 11. Initial matric suction condition for edge lift mode of analysis

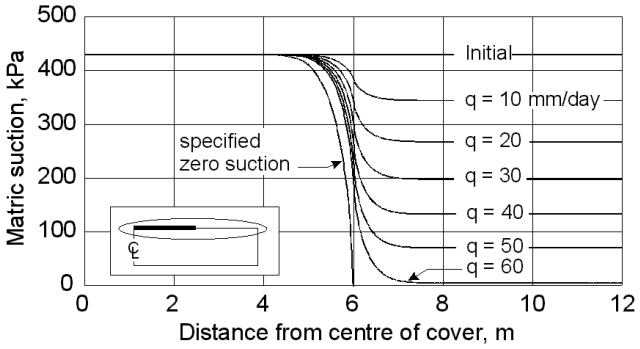

Figure 12. Matric suction at ground surface after one day of infiltration for various infiltration rates

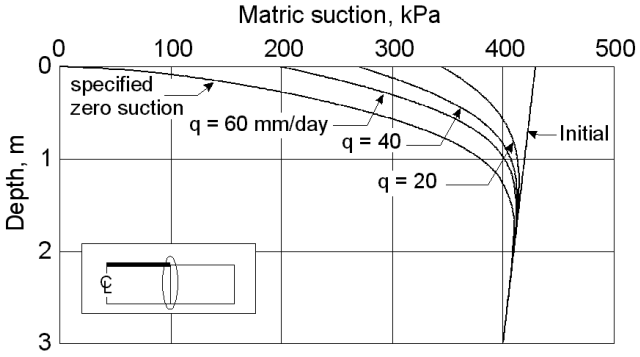

Figure 13. Matric suction profile at the edge of the cover after one day of infiltration for various infiltration rates

Figures 14, 15 and 16 present the results of a transient seepage analysis for the case where zero suction is specified at the exposed boundary. Figure 14 shows the contours of matric suction after one day of infiltration. It can be seen that most suction change took place only in the upper right portion of the soil domain. Figure 15 shows the changes of suction with time at various monitoring points in the soil mass. Suction decreased significantly near the uncovered ground surface in the first 25 days of infiltration, and approached a steady state condition in about 50 days. Figure 16 presents the matric suction profiles at the edge of the cover for various times during the transient process and at steady state conditions. Most of the suction change occurred early after infiltration commenced.

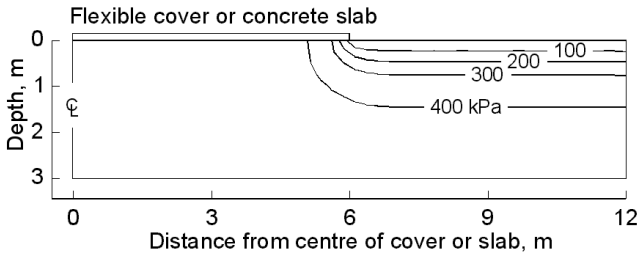

Figure 14. Matric suction distribution after one day of infiltration when zero suction is specified at the uncovered boundary

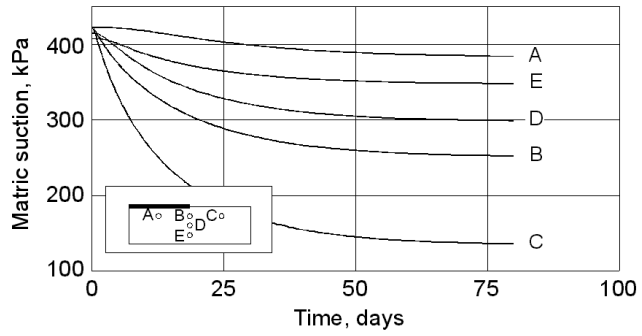

Figure 15. Change of suction with time at various points in soil when zero suction is specified at the uncovered boundary

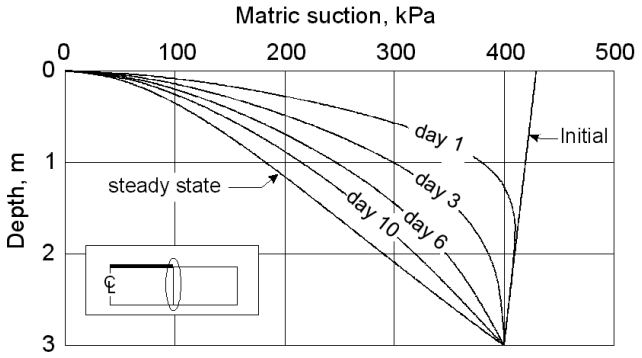

Figure 16. Matric suction profiles at the edge of the cover for various elapsed times when zero suction is specified at the uncovered boundary

Figures 17 and 18 present the vertical displacements at ground surface and the vertical displacements versus depth at the edge of the cover, respectively, after one day of infiltration corresponding to various infiltration rates. It is obvious that differential movements at this time took place only near the edge of the cover, where there is a change in matric suction. Insignificant movements (i.e., less than 1 mm) were observed under the inside portion of the cover. The differential movement increased with an increasing rate of infiltration, and maximized at about 20 mm for the case when zero suction was specified at the uncovered boundary. Again, most displacement in soils took place near ground surface.

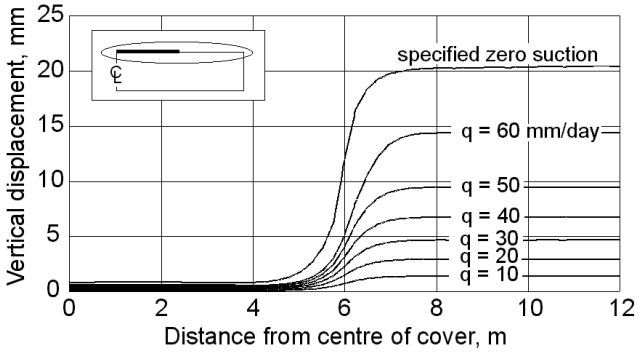

Figure 17. Vertical displacements at ground surface (with flexible cover) after one day of infiltration for various infiltration rates

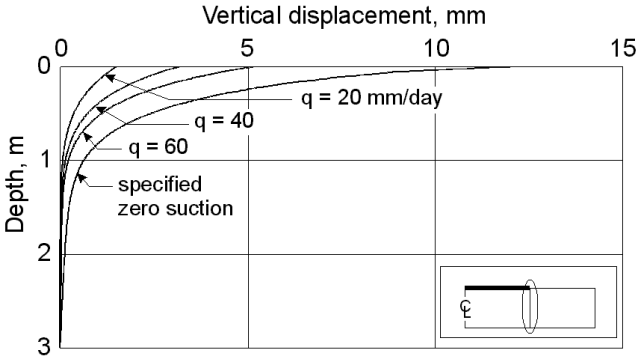

Figure 18. Vertical displacement versus depth at the edge of the flexible cover after one day of infiltration for various infiltration rates

Edge lift for a slab of uniform thickness

This scenario is similar to the edge lift involving a flexible cover presented previously, the difference is that a slab of 10-cm thickness is placed instead of the flexible cover and there are loads applied in the interior and perimeter of the slab. Deformation in the slab and soil due to applied load and wetting is analyzed. A load of 0.5 kPa is applied on the interior of the slab and a load of 10 kN/m is applied on the perimeter of the slab. The results of seepage analysis were presented previously in Figs. 11, 12, 13, 14 and 15. Deformation in the slab and soil mass due to loading can be assumed to respond immediately, while the deformation due to wetting is a time dependent process.

Figure 19 presents the vertical displacements of the slab after loading and wetting with times. The maximum displacements are predicted when the matric suction condition in the soil corresponds to that of a steady state condition. The largest displacement of the slab occurred at the edge. The edge of the slab first bent down due to perimeter load, then bounded up due to swelling of the underlying soil. The displacement at the edge of the slab increased with time and reached a maximum value of 30 mm when suction approached a steady state condition. These maximum cumulative vertical displacements in soil are presented in Fig. 20. A maximum total heave of about 60 mm was computed at surface, outside of the slab.

The results of the stress-deformation analysis also include the distribution of the resulting stresses in the slab. Figure 21 shows the flexural stresses at the top and bottom of the slab corresponding to the maximum vertical displacements. The bending moments occurred after loading and each of the wetting periods are presented in Fig. 22. Negative moments occurred as a result of the externally applied loads. Positive moments resulted due to swelling of the soil around the edge of the cover. Figure 23 presents the cumulative bending moments for various elapsed times after loading and wetting. It can be observed that the bending moments increased rapidly, peaked, and decreased gradually as the distance from the edge of the slab increases. This pattern of moment distribution agrees with that presented in Warren (1978) and Post-Tensioning Institute manual (1996).

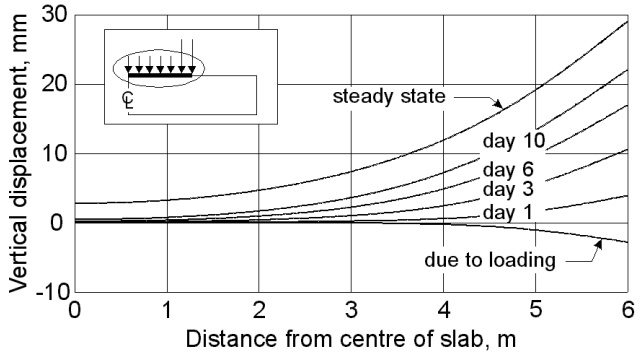

Figure 19. Vertical displacement of the slab after loading and wetting with times

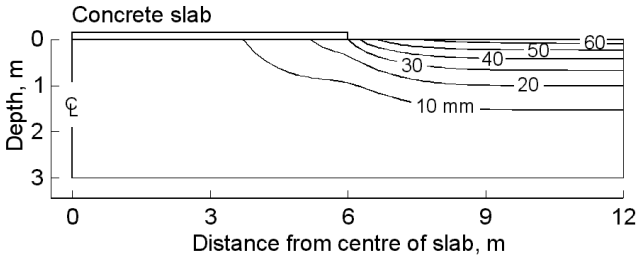

Figure 20. Contours of vertical displacements at steady state condition when zero suction is specified

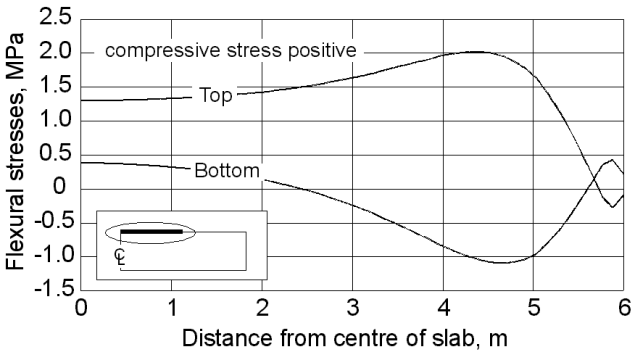

Figure 21. Flexural stresses at top and bottom of the slab at steady state suction condition

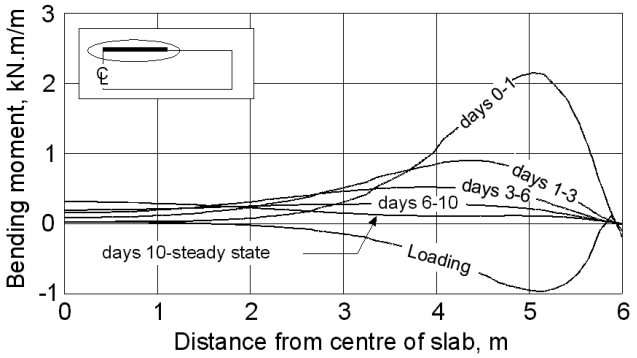

Figure 22. Bending moments due to loading and each period of wetting

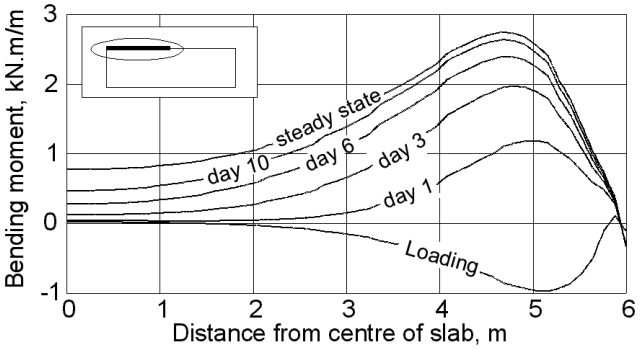

Figure 23. Cumulative bending moments after loading and various elapsed times of wetting

CONCLUDING REMARKS

The presented numerical models have been developed based on general theory for unsaturated soil behaviour. Predicted responses of the soil to moisture flux boundary conditions are consistent with those generally observed in the field. The saturated/unsaturated seepage and stress/deformation models presented in this paper appeared to be potential tools for the analysis of swelling and shrinking soils underlying slabs-on-ground constructed on unsaturated soils. The analyses shown in this paper can be extended to accommodate the analysis of slab-on-ground problems in three dimensions.

REFERENCE

Fredlund, D.G. and Hung, V.Q. 2001. Prediction of Volume Change in an Expansive Soil as a Result of Vegetation and Environmental Changes. Proceedings of the Civil Engineering Conference on Expansive Soils and Vegetative Effects on Shallow Foundations, Houston, TX, USA, pp. 24-43.

Fredlund D.G., and Morgenstern, N.R. 1977. Stress State Variables for Unsaturated Soils. ASCE Journal of Geotechnical Engineering, 103: 447-466.

Fredlund, D.G. and Rahardjo, H. 1993. Soil Mechanics for Unsaturated Soils. John Wiley & Sons, New York, 560 p.

Fredlund, D.G. and Xing, A. 1994. Equation for the Soil-Water Characteristic Curve. Canadian Geotechnical Journal, 31(3): 521-532.

Fredlund, D.G., Xing, A., and Huang, S. 1994. Predicting the Permeability Function for Unsaturated Soils using the Soil-Water Characteristic Curve, Canadian Geotechnical Journal, 31(3): 533-546.

Gardner, W.R. 1958. Some Steady State Solutions of Unsaturated Moisture Flow Equation with Application to Evaporation from a Water Table. Soil Science, 85: 228-232.

Hung , V.Q. 2003. Uncoupled and coupled solutions of volume change problems in expansive soils, Ph.D. dissertation, University of Saskatchewan, Saskatoon, SK, Canada, 329 p.

Hung, V.Q., and Fredlund, D.G. 2000. Volume Change Prediction in Expansive Soils Using a Two-dimensional Finite Element Method, Proceeding of the Asian Conference on Unsaturated Soils, Singapore, pp. 231-236.

Leong, E.C. and Rahardjo, H. 1997. Permeability Functions for Unsaturated Soils. Journal of Geotechnical and Geoenvironmental Engineering, ASCE, pp: 1118-1126.

Lytton, R.L. 1995. Foundations and pavements on Unsaturated Soils, Proceedings of the first International Conference on Unsaturated Soils, Paris, Vol. 3, pp. 1201-1220.

Lytton, R.L. 1997. Engineering Structures in Expansive Soils, Keynote Address, Proceedings of the third International Symposium on Unsaturated Soils, Rio de Janeiro, Brazil.

Post-Tensioning Institute. 1996. Design and construction of post-tensioned slabs-on-ground, Second edition, 101 p.

Timoshenko, S., and Woinowsky-Krieger, S. 1959. Theory of Plates and Shells, McGraw-Hill, 580 p.

van Genuchten, M.T. 1980. A Closed-formed Equation for Predicting the Hydraulic Conductivity of Unsaturated Soils. Soil Science Society of America Journal, 44: 892-898.

Warren K. W. 1978. Development of a design procedure for residential and light commercial slabs-on-ground constructed over expansive soils. Ph.D. dissertation, Volume 1, Texas A & M University, College Station, Texas, USA, 241 p.